TISSUE ENGINEERING: Part A
Volume 17, Numbers 21 and 22, 2011

DOI: 10.1089/ten.tea.2010.0533

A Healing Method of Tympanic Membrane Perforations Using Three-Dimensional Porous Chitosan Scaffolds

Jangho Kim, M.S.,[1,2] Seung Won Kim, M.D.,[3] Seong Jun Choi, M.D.,[4] Ki Taek Lim, M.S.,[1] Jong Bin Lee, M.D.,[4] Hoon Seonwoo, B.S.,[1] Pill-Hoon Choung, D.D.S., Ph.D.,[5] Keehyun Park, M.D., Ph.D.,[3] Chong-Su Cho, Ph.D.,[2] Yun-Hoon Choung, D.D.S., M.D., Ph.D.,[3] and Jong Hoon Chung, Ph.D.[1,2]

Both surgical tympanoplasty and paper patch grafts are frequently procedured to heal tympanic membrane (TM) perforation or chronic otitis media, despite their many disadvantages. In this study, we report a new healing method of TM perforation by using three-dimensional (3D) porous chitosan scaffolds (3D chitosan scaffolds) as an alternative method to surgical treatment or paper patch graft. Various 3D chitosan scaffolds were prepared; and the structural characteristics, mechanical property, *in vitro* biocompatibility, and healing effects of the 3D chitosan scaffolds as an artificial TM in *in vivo* animal studies were investigated. A 3D chitosan scaffold of 5 wt.% chitosan concentration showed good proliferation of TM cells in an *in vitro* study, as well as suitable structural characteristics and mechanical property, as compared with either 1% or 3% chitosan. In *in vivo* animal studies, 3D chitosan scaffold were able to migrate through the pores and surfaces of TM cells, thus leading to more effective TM regeneration than paper patch technique. Histological observations demonstrated that the regenerated TM with the 3D chitosan scaffold consisted of three (epidermal, connective tissue, and mucosal) layers and were thicker than normal TMs. The 3D chitosan scaffold technique may be an optimal healing method used in lieu of surgical tympanoplasty in certain cases to heal perforated TMs.

Introduction

Tympanic membrane (TM) perforation occurring over time is a common problem in otology, and chronic otitis media is also one of the most critical otologic diseases. TM perforations, caused by infection or physical external trauma to the middle ear, usually present conductive healing loss and chronic infections.[1] Although most acute TM perforations heal spontaneously due to the prominent regeneration capacity of the TM, large TM perforations or those combined with chronic otorrhea or inflammation do not heal without specific surgical treatments, such as an autologous autograft from the muscle fascia or perichondrium. In most studies, these surgical treatments have shown a success rate between 88% and 97% for healing TM perforations. However, surgical treatments have many limitations: (1) high cost of the operation, (2) defective donor sites, (3) the need for general anesthesia in some patients, (4) complex microsurgical skills of the surgeon, and (5) aseptic procedures.[2,3]

A paper patch technique, first introduced by Blake, is a very famous method used to heal TM perforations without surgical treatment. In this technique, a paper patch plays a role in guiding the epithelial cells to migrate around the border of the perforation. This technique has been frequently used to treat acute and traumatic perforations in out-patient clinics. However, a number of studies have reported that the paper patch technique has many disadvantages and limitations for healing TM perforations in clinical practice. First of all, paper patch technique is not the upmost promising procedure of 100% healing rate for TM perforations. Further, paper patches used to heal TM perforations have several limitations, such as nontransparency, nonflexibility, easy detachment, and nonresistance to infection, which complicates the healing of TM perforations.[1–5]

With recent rapid advances in regenerative medicine fields related to biomaterials, tissue engineering, drug delivery, and stem cell therapy, novel methods to heal TM perforations have been studied as alternatives to surgical repairs of TM perforations. Many researchers have attempted to regenerate TM using biomaterials, such as collagen,[6] hyaluronic acid,[7] Poly(B-benzyl-L-aspartate-co-L-leucine)50/50,[8]

[1]Department of Biosystems & Biomaterials Science and Engineering, Seoul National University, Seoul, Republic of Korea.
[2]Research Institute for Agriculture and Life Sciences, Seoul National University, Seoul, Republic of Korea.
[3]Department of Otolaryngology, Ajou University School of Medicine, Suwon, Republic of Korea.
[4]Department of Otolaryngology, College of Medicine, Konyang University, Daejeon, Republic of Korea.
[5]Tooth Bioengineering National Research Lab, Department of Oral and Maxillofacial Surgery, School of Dentistry, Seoul National University, Seoul, Republic of Korea.

calcium alginate,[9] silk,[10,11] chitosan,[3,12] AlloDerm,[2] or urinary bladder matrix,[13] which is based on the paper patch technique. These studies demonstrated that biomaterials as an artificial TM patch may play a role in potential therapy for healing TM perforations without surgical treatments. These artificial TM patches showed a very high closure ratio in cases of the acute TM. Still, the regeneration efficacy is being challenged in the cases of chronic TM perforations. Drug delivery therapies using epidermal growth factor, basic fibroblast growth factor (bFGF),[7] or pentoxifyline (Trental)[14] have also been studied experimentally for TM regeneration. Hakuba *et al.* tried to combine bFGF and an artificial patch to repair TM perforations.[15] In addition, recent novel therapies based on tissue engineering[10,16,17] and stem cell techniques[18–20] have been reported by some research groups. Up to date, many studies and methods have shown high potential for TM regeneration; however, no definite treatment regarding alternatives to surgical or the paper patch technique for clinical applications have been reported.

We believe that the ideal therapy for healing TM perforations as an alternative to surgical treatment should satisfy the following properties: (1) high closure ratio of TM perforations in both acute and chronic cases, (2) simple treatment to heal TM perforations with a short TM healing period, and (3) low treatment cost. Herein, we report a new healing method for TM perforations using three-dimensional (3D) porous scaffolds as a potential candidate for clinical application of TM regeneration. The traditional paper patch technique including artificial patches is that patches guide TM cells to regenerate along surface of the patch. The new method we report here is that the 3D porous scaffold is grafted into a perforated TM guiding TM cells to effectively regenerate along its surface and pores. For choosing the biomaterial for fabricating the 3D porous scaffolds in this study, we selected the chitosan among many biomaterials because of its biocompatibility, biodegradable property, wound-healing accelerator, antibacterial property, and ease of processing. In particular, a number of studies demonstrated that the 3D porous scaffolds fabricated by both water-insoluble chitosan and water-soluble chitosan were very effective for tissue-engineering applications such as bone, skin, cartilage, liver, nerve, and blood vessel *in vitro* and *in vivo*.[21–23] Further, we have previously reported that both water-insoluble chitosan and water-soluble chitosan as a material of the artificial patch were effective for TM regeneration, indicating that both water-insoluble chitosan and water-soluble chitosan would be good candidates as a platform for the application of TM regeneration.[3,12] In this study, we used water-insoluble chitosan as a main source for fabricating the 3D porous scaffolds due to their ability to maintain their 3D structure properties during TM regeneration period as well as biocompatibility for TM regeneration. However, 3D scaffolds fabricated by water-soluble chitosan might collapse because of their water-soluble property even before TM regeneration in the external ear canal, eventually losing their 3D porous structure. Thus, we fabricated 3D porous chitosan scaffolds (3D chitosan scaffolds) as a novel artificial TM using water-insoluble chitosan, investigated their properties, and evaluated the TM healing effects in *in vitro* and *in vivo* studies.

Materials and Methods

Materials

Chitosan (molecular weight: 200,000, deacetylation degree: 89%) was purchased from Taehoon Company. The paper patches were hand made from the cigarette paper in the outpatient clinic and sterilized with ethylene oxide gas. Primary TM cells were obtained from TMs of 5 day-old Sprague-Dawley rats under the anesthesia with 0.025 mL/g avertin (1.25% tribromoethanol, intraperitoneal injection), and the TM cells were cultured and maintained at 37°C in Dulbecco's modified Eagle's medium (DMEM) supplemented with 10% fetal bovine serum (FBS) in a humidified atmosphere with 5% CO_2 for 2 weeks for *in vitro* study. The culture media (DMEM), FBS, EDTA, and 3-(4, 5-dimethyl-2-thiazoly (2.5-d-iphenyl-2H-terazolium bromide)) (MTT) were purchased from Sigma-Aldrich.

Fabrication of 3D chitosan scaffolds

3D chitosan scaffolds were fabricated as previously reported.[24] Briefly, chitosan solutions with concentrations of 1%, 3%, and 5 wt.% were prepared with distilled water in 1 wt.% acetic acid. Freezing and lyophilizing of chitosan solutions in cylindrical molds (diameter: 5 mm, height: 2.5 mm) were used to fabricate 3D chitosan scaffolds (Fig. 1A). Freezing of chitosan solutions was accomplished by immersing the cylindrical molds in freezing baths maintained at −20°C. The samples were then lyophilized until dried. The prepared samples were neutralized with ethanol for overnight and subsequently washed using phosphate-buffered saline (PBS). We prepared the 3D chitosan scaffolds as a novel artificial TM with large pores by cutting the initial 3D chitosan scaffolds with a knife after briefly freezing the samples with liquid nitrogen (Fig. 1B, C).

Morphological observation of 3D chitosan scaffolds

Morphologies of surface and cross-sections of the 3D chitosan scaffolds were gold-coated and observed with a field-emission scanning electron microscope (FESEM; JEOL, JSM-5410LV) at an accelerating voltage of 2 kV. First, we observed the initial 3D chitosan scaffolds using FESEM. After cutting the initial 3D chitosan scaffolds for an artificial TM, we also studied the morphology of the 3D chitosan scaffold using FESEM. After obtaining the FESEM images, 5 images of each 3D chitosan scaffold according to the concentrations of chitosan were used to quantify the pore sizes of the 3D chitosan scaffolds using Adobe Photoshop software (Adobe). Briefly, 10 to 20 pores from 10 to 20 in each FESEM image were employed to determine the mean pore size of the 3D chitosan scaffolds.

Mechanical properties of 3D chitosan scaffolds

The 3D chitosan scaffolds (diameter: 5 mm, height: 2.5 mm) were prepared to measure their mechanical properties. The compressive strength of the 3D chitosan scaffolds were measured by a texture analyzer (Stable Micro Systems Ltd.), and the cross-head speed was set at 10 mm/min. These tests were repeated five times, and the peak load and breaking point displacement were recorded. The modulus of the 3D chitosan scaffolds were calculated by the slope of the linear region in the stress-strain curves.

In vitro *proliferation study of TM cells in 3D chitosan scaffolds*

We investigated *in vitro* proliferation study of TM cells in the 3D chitosan scaffolds using the previously reported procedure.[25] Briefly, 300 μL of chitosan solutions were poured into 24-well culture plates; and then, they were frozen at −20°C and lyophilized. The samples were neutralized with ethanol for overnight and subsequently washed using PBS. The TM cells were seeded at a density of 1.5×10^4 cells/well into the samples. Cell viability was determined with an MTT assay at 0, 1, 3, and 5 days after TM cell seeding. For the MTT assay, the samples were washed twice using PBS; 200 μL of 5 mg/mL MTT solution was added to each well, and the samples were incubated at 37°C and 5% CO_2 for 4 h. After incubation, the MTT solution was removed, and 500 μL of dimethyl sulfoxide was added to dissolve the formazan crystals. Absorbance was measured at 570 nm using a microplate reader (VERSAMAX Reader; Molecular Devices). The *in vitro* cell growth in the 3D chitosan scaffold was also observed by a FESEM. The 3D chitosan scaffolds (diameter: 5 mm, height: 2.5 mm) were prepared. The sample was placed in 24-well culture plates, and the TM cells were seeded at a density of 2×10^4 cells/scaffold. After 5 days of cell seeding, samples were fixed with modified Karnovsky's fixative (2% paraformaldehyde and 2% glutaraldehyde in 0.05 M sodium cacodylate buffer) for 4 h. The samples were washed thrice with 0.05 M sodium cacodylate buffer for 10 min. The samples were washed with distilled water and dehydrated with graded concentrations (50%, 70%, 80%, 90%, and 100% v/v) of ethanol. The samples were treated with hexamethyldisilazane for 15 min. Finally, the samples were coated with gold for cell morphology observation using FESEM.

In vivo *animal study*

Sprague-Dawley rats (12 weeks, 250–300 g) were anesthetized with chloral hydrate (1 g/mL, 10% dilution). Mechanical perforations were made ~40%–50% in size on the anterior half area of both TMs using a micropick under a surgical microscope (Fig. 4B, G). The perorated TM sizes were checked using Adobe Photoshop software (Adobe). As a result, we knew that the perforated TM sizes were 42.8% ± 4.4% (for *in vivo* animal study for the 3D chitosan scaffolds, $n=10$) and 42.5% ± 4.3% (for *in vivo* animal study for the paper patches, $n=10$) in size, indicating that the *in vivo* animal models for TM regeneration study were well prepared. The 3D chitosan scaffolds were grafted to the right perforated TMs of rats (Fig. 4C). As a control group, the paper patches were applied to the left perforated TMs of rats (Fig. 4H). Ofloxacin ointment (Tarivid® ophthalmic ointment; Santen Pharmaceutical Company), was applied to the scaffold to contact the entire margin of perforation. To control bleeding during the procedure, a gelatin sponge (Cutanplast®; Mascia Brunelli) was used. The healing states of the perforated TMs were checked at 3, 7, 10, and 14 days under a surgical microscope (Fig. 4A–K).

Assessment of hearing study

Auditory brainstem response (ABR) was performed before TM perforation and after TM regeneration with 3D chitosan scaffolds. Rats were anesthetized as previously described. ABR was measured for both ears of each animal at 16 and 32 kHz. A differential active needle electrode was placed subcutaneously below the tested ear, a reference electrode at the vertex, and a ground electrode below the contralateral ear. ABRs were recorded by using an evoked potential averaging system (Tucker-Davis Technologies) in an electrically shielded, sound-treated booth in response to tone bursts at 16 and 32 kHz. For each stimulus, electroencephalographic activity was recorded for 20 ms at a sampling rate of 25 kHz, filtered (0.3–3 kHz), and waveforms from 512 stimuli were averaged for click responses, and 1000 stimuli for frequency-specific stimuli (8, 16, and 32 kHz). ABR waveforms were recorded in 5 dB sound pressure level intervals down from the maximum amplitude. Threshold by visual inspection was defined as the lowest stimulus level at which response peaks for wave I–V were clearly present. The mean value of thresholds checked by visual inspection and computer analysis was defined as ABR threshold at each stimulus. Data were obtained from each group.

Histological observations

Two weeks after treatment with 3D chitosan scaffolds and paper patches, if the TMs had healed completely, then 5 mL chloral hydrate (1g/mL, 10% dilution) was injected intraperitoneally to sacrifice the rats. Tympanic bulla were obtained immediately from the heads of the rats and fixed in formaldehyde. Some specimens were decalcified in formic acid for 2 weeks, and cross-sectional findings were stained with hematoxylin and eosin, along with examination under an optical microscope. Four or 8 weeks after treatment with 3D chitosan scaffolds, we also observed the TM regenerated using a transmission electron microscopy (TEM; EM 902A, Zeiss).

Statistical analysis

Statistical analyses were performed using the Statistical Analysis System (SAS) for Windows Ver. 8.2 (SAS Institute) and SPSS (SPSS Inc.). Duncan's multiple range test was used to compare the means of the properties of the 3D chitosan scaffolds using a Statistical Analysis System (SAS) for Windows Ver. 8.2 (SAS Institute). The Kruskal–Wallis one-way analysis of variance was used to compare the *in vitro* proliferation of TM cells in the 3D chitosan scaffolds. The comparison of treatment results of traumatic-perforated TMs between 3D chitosan scaffolds and paper patches were analyzed using the chi-square test with SPSS. The level of significance was $p<0.05$.

Results and Discussion

Fabrication and characteristics of 3D chitosan scaffold as a novel artificial TM

The basic concept of the new healing method of TM perforations using a 3D chitosan scaffold is shown in Figure 1D. The microstructures of a scaffold, such as size, shape, and pore distribution, are very important for artificial TMs, because they allow cells to be effectively regenerated along the surface or into the pores of the artificial TMs. Thus, artificial TMs have to provide a suitable structure during TM regeneration. Due to thermal gradients of chitosan solutions during freezing and lyophilizing for fabrication of 3D chitosan scaffolds, the pore sizes in the initial 3D chitosan scaffolds

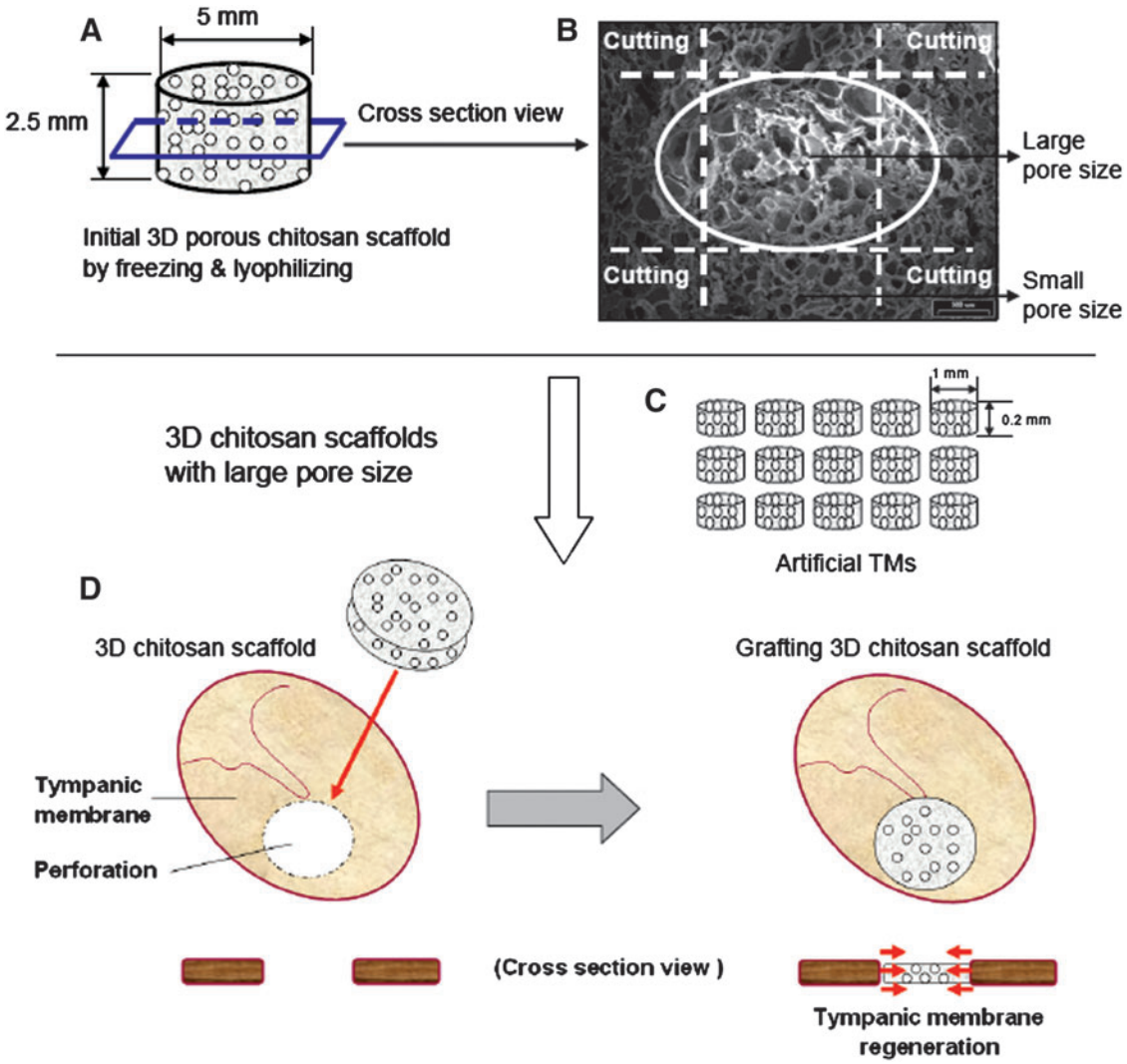

FIG. 1. A new method of TM regeneration using a 3D chitosan scaffold. **(A)** Initial 3D chitosan scaffolds (diameter: 5 mm, height: 2.5 mm) made by freezing and lyophilizing. **(B)** Cross-sectional view of initial 3D chitosan scaffolds (SEM image); the initial 3D chitosan scaffolds had various pore sizes, due to thermal gradients of chitosan solutions during freezing and lyophilizing. **(C)** The 3D chitosan scaffolds as an artificial TM that were prepared by cutting the initial 3D chitosan scaffolds. **(D)** Basic concept of TM regeneration using a 3D chitosan scaffold; the grafted 3D chitosan scaffold guides TM regeneration. TM, tympanic membrane; 3D, three-dimensional. Color images available online at www.liebertonline.com/tea

were different[26] (Fig. 1B and Supplementary Fig. S1; Supplementary Data are available online at www.liebertonline.com/tea). In particular, the center region of the initial 3D chitosan scaffolds showed larger pore sizes than the other regions (Supplementary Fig. S1). Since 3D scaffolds with very small pore sizes may be interrupted by proliferation or migration of TM cells and those with larger pore sizes would easily support the actions, we predicted that the center region of initial 3D chitosan scaffolds would be more suitable as an artificial TM than the other regions. We prepared a 3D chitosan scaffold with large pore sizes as a novel artificial TM by cutting the initial 3D chitosan with a cutting knife a moment after freezing in liquid nitrogen (Fig. 1C).

The cross-sectional morphologies of the 3D chitosan scaffolds prepared using different concentrations of chitosan are shown in Figures 2A–C. The pore sizes on the 3D chitosan and the pore sizes in the cross-sectioned areas ranged from 143.9 ± 29.7 to $230.5 \pm 28.4\,\mu m$, respectively, according to the concentration of chitosan (Fig. 2D). The average pore size on the cross-sectioned areas of the 3D chitosan scaffolds showed a tendency to decrease with an increased concentration of chitosan, because high concentrations of chitosan have higher viscosity, and lyophilizing maintained the smaller pore size.[26] We also learned that the pores of the 3D chitosan scaffolds were highly interconnected with one another. The 3D chitosan scaffolds as artificial TMs had adequate pore size, shape, and pore distribution, regardless of the concentration of chitosan, indicating that these scaffolds would be effective for TM regeneration.

The compressive strengths, stress-strain relationship, and the compressive modulus of the 3D chitosan scaffolds are shown in Figure 2E and F. The compressive strength of the 3D chitosan scaffolds showed a tendency to increase depending on the concentration of chitosan. The compressive

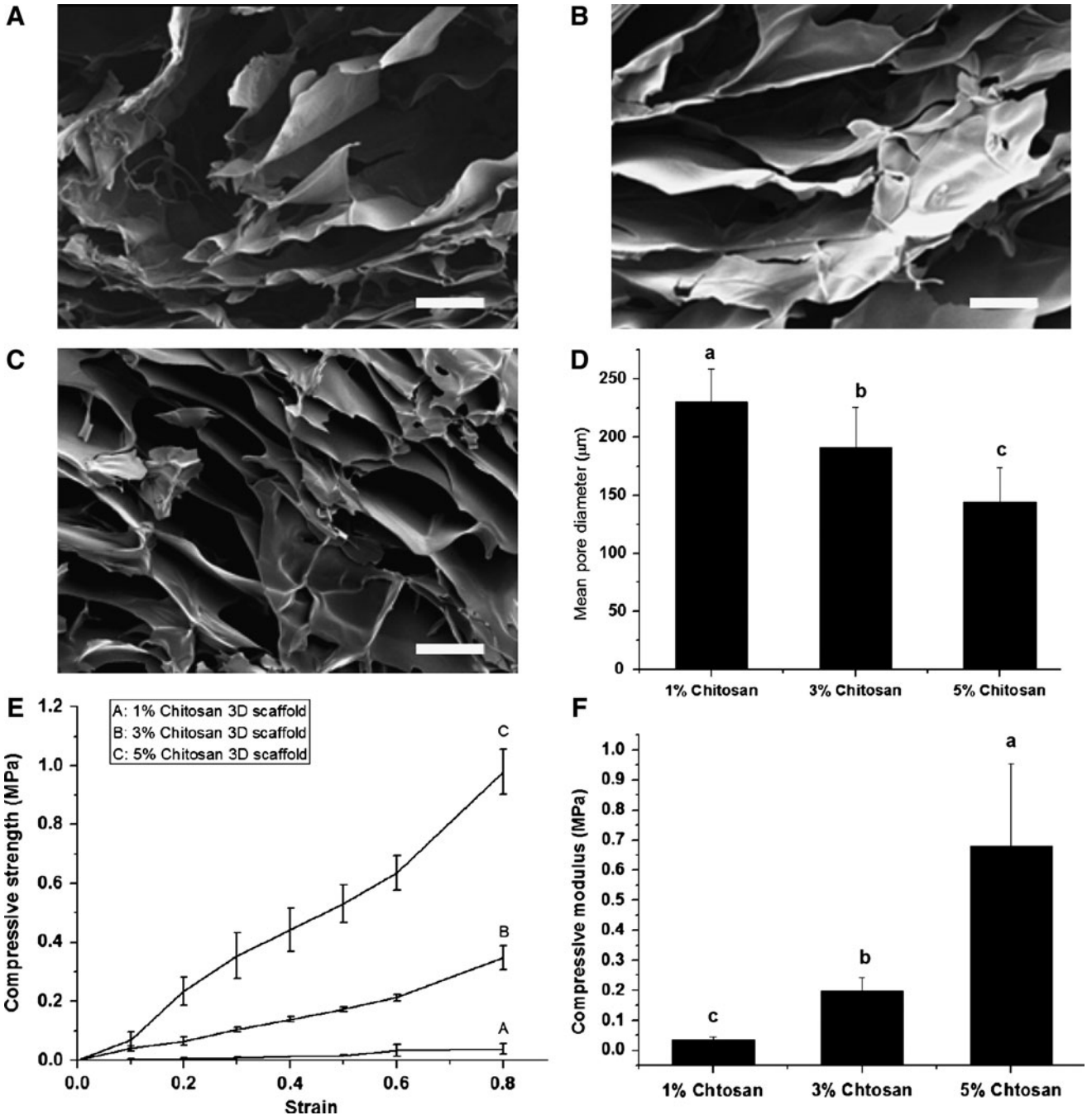

FIG. 2. Characteristics of the 3D chitosan scaffolds. (A-C) FESEM images of structure of the 3D chitosan scaffolds with different concentrations of chitosan. **(A)** 1 wt.% concentration of chitosan. **(B)** 3 wt.% concentration of chitosan. **(C)** 5 wt.% concentration of chitosan. **(D)** Quantification of average pore diameters of the 3D chitosan scaffolds according to the different concentrations of chitosan ("a–c" mean that the average pore diameters of the 3D chitosan scaffolds are significantly different among different characters [$p < 0.05$, $n = 5$ for each group)]. **(E)** Stress-strain diagram of the 3D chitosan scaffolds. **(F)** Compressive modulus of the 3D chitosan scaffolds ("a–c" mean that the compressive modulus of the 3D chitosan scaffolds are significantly different among different characters [$p < 0.05$, $n = 3$ for each group]). Error bars in **(D–F)** represent the SD about mean. Scale bars = 100 μm. FESEM, field-emission scanning electron microscope.

modulus of the 3D chitosan scaffolds ranged from 0.0366 ± 0.0084 to 0.6813 ± 0.2732 MPa, depending on the concentration of chitosan. The 5 wt.% 3D chitosan scaffolds had the highest mechanical strength, although they had small pore sizes, as compared with the other two 3D chitosan scaffolds with different chitosan concentrations.

In vitro *proliferation of TM cells in 3D chitosan scaffolds*

The TM is composed of keratinocytes and fibroblasts. We analyzed the composition ratio of these cells using fluorescence-activated cell sorting. The fibroblasts constituted >95% of the total cell number and keratinocytes

(epithelial cells) around 0.1% (data not shown). Accordingly, fibroblasts were considered as the main cells involved in the regeneration of the perforated TMs growing along the epithelial cells.

The TM cells were seeded into the 3D chitosan scaffolds and tissue culture polystyrene (TCPS) dishes as a positive control. After removing the unattached TM cells by PBS washing, the viability of TM cells in the 3D chitosan scaffolds was quantified by MTT assay. The TM cell viability in the 3D chitosan scaffolds and TCPS dishes is shown in Figure 3A and indicates that the 3D chitosan scaffolds, regardless of the chitosan concentrations, provided a suitable environment for TM regeneration although the TM cell viability on the TCPS dishes as a positive control was higher than those of the 3D chitosan scaffolds. We also observed proliferation in all TM cells with 3D chitosan scaffold regardless of the chitosan concentration, concluding that 3D chitosan scaffold is a suitable candidate for artificial TM for TM regeneration.

To confirm the grown TM cells in the 3D chitosan scaffolds, we checked the FESEM observation of the 3D chitosan scaffolds after 5 days of TM cell culture. Figure 3B shows that the TM cells were adhered and spread properly in the surface of the 3D chitosan scaffolds. We also observed that the TM cells were well grown in the cross-section of the 3D chitosan scaffolds (Fig. 3C). Interestingly, the TM cells were spread horizontality or vertically in the 3D chitosan scaffolds. Basically, the 3D chitosan scaffolds provided suitable 3D structure environment for TM cells.

With these *in vitro* study findings, we are able consider all 3D chitosan scaffolds as an applicable biomaterial for artificial TMs. In our previous studies, we also demonstrated the features of chitosan as an excellent biocompatible biomaterial for TM cells *in vitro*.[3,12]

Selection of 3D chitosan scaffold for in vivo *applications*

We prepared various 3D chitosan scaffolds for new artificial TMs. The characteristics and *in vitro* studies suggest that all of the 3D chitosan scaffolds fabricated were suitable as artificial TMs. However, we had to consider the mechanical properties of the 3D chitosan scaffolds for *in vivo* applications, because the 3D chitosan scaffold should play a role as a temporary TM during the TM regeneration period. The artificial TMs should have good mechanical strength so that they could provide a good environment for supporting TM cell growth and proliferation, as well as allowing sound transmission during the period of TM regeneration. The 5 wt.% 3D chitosan scaffolds had the highest mechanical strength, as compared with the other two concentrations, due to its high chitosan content. Further, they showed the suitable TM cell viability, as well as the suitable pore size, shape, and distribution of pores. Therefore, we decided that the 3D chitosan scaffold of concentration of 5 wt.% chitosan was the best candidate among several candidates for an artificial TM and studied the TM regeneration effect through *in vivo* animal studies.

In vivo *animal study*

We continued to use the 5 wt.% chitosan 3D chitosan scaffold for our *in vivo* animal studies. Ten Sprague-Dawley rats with perforated TMs were prepared. After microscopic examination confirming TM perforation (Fig. 4B, G), we grafted 5 wt.% chitosan 3D chitosan scaffolds into the rats' perforated TMs (Fig. 4C) and applied the paper patches into the other group (Fig. 4H). For 14 days, the individual changes of perforated TM and the maintenance rate of perforations in each group were measured (Fig. 4L, M). After 3 days,

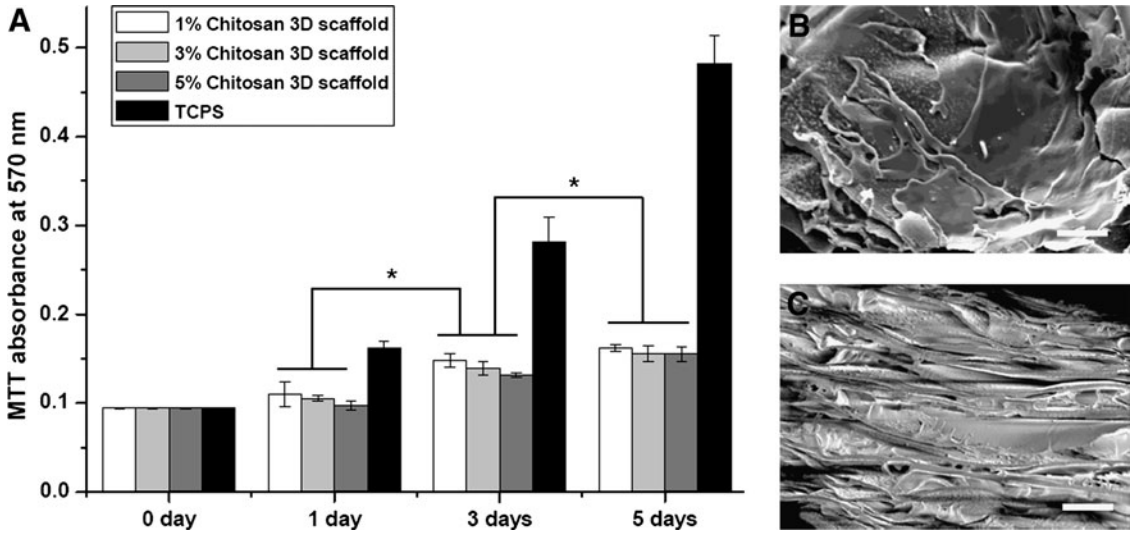

FIG. 3. *In vitro* study for proliferation of TM cells in the 3D chitosan scaffolds. **(A)** The cell viability of TM cells on the 3D chitosan scaffolds with different concentrations of chitosan and TCPS dishes at 0, 1, 3, and 5 days after TM cell seeding. **(B, C)** FESEM images of TM cells cultured on the 3D chitosan scaffolds (5 wt.% concentration of chitosan); After being cultured for 5 days, the TM cells were well adhered and densely populated in **(B)** the surface area of the 3D chitosan scaffold and **(C)** the cross sectional area of the 3D chitosan scaffold. Error bar in **(A)** represents the SD about the means ($*p < 0.05$, $n = 3$, Kruskal–Wallis one-way analysis of variance). Scale bars = 100 μm. TCPS, tissue culture polystyrene.

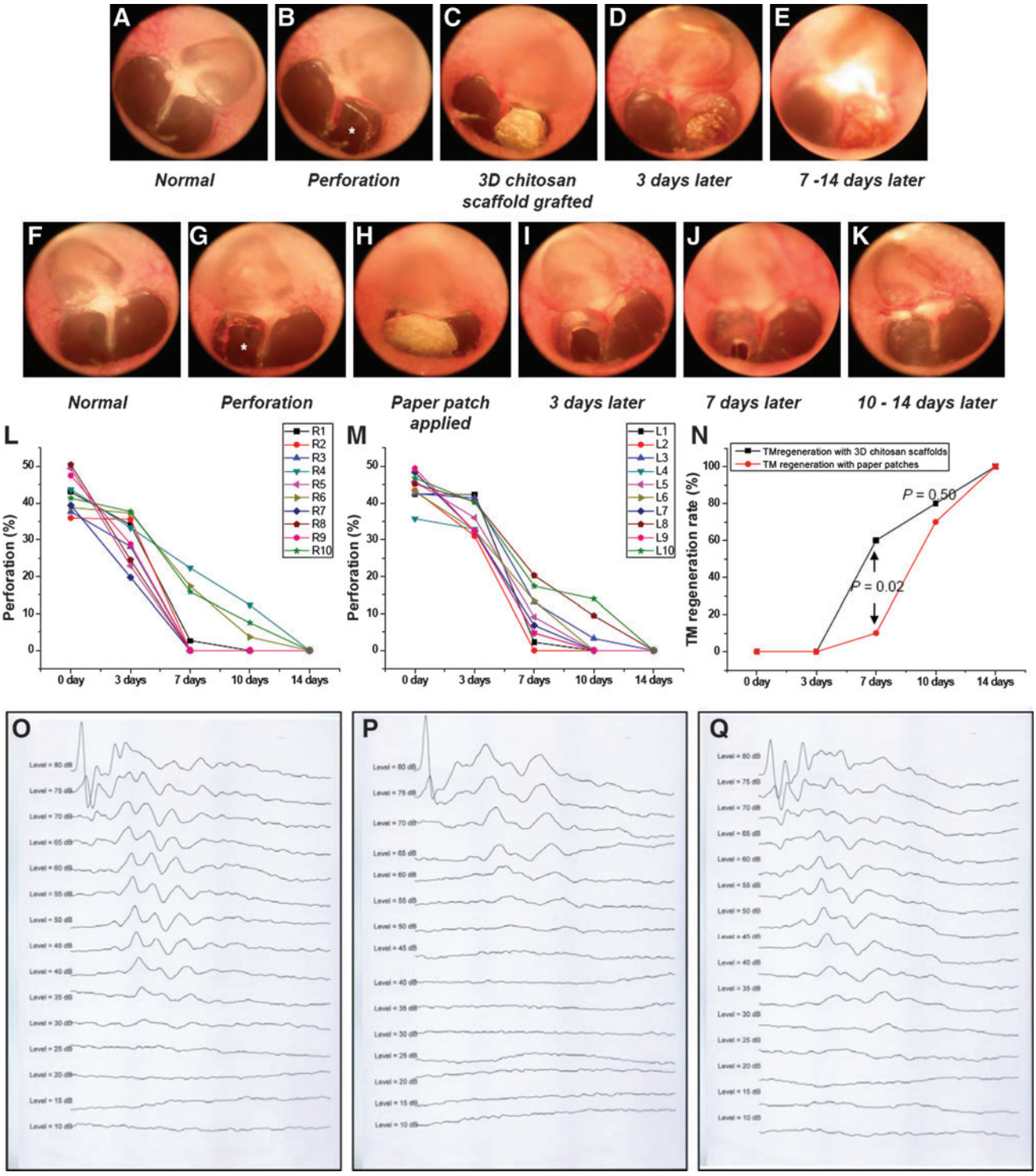

FIG. 4. *In vivo* model animal study of TM regeneration using **(A–E)** the 3D chitosan scaffolds and **(F–K)** the paper patches after perforation (*) of TMs. The individual changes of perforated TMs in each group **(L**, 3D chitosan scaffold group; **M**, paper patch group**)** were observed for 14 days. **(N)** shows a statistical comparison (chi-square test) of a perforated TM recovery using the 3D chitosan scaffolds and paper patches. Typical results of auditory brainstem response (ABR) tests of **(O)** the normal TM rats and **(P)** the perforated TM rats, and **(Q)** the regenerated TM rats with the 3D chitosan scaffolds; the ABR tests indicate that the hearing ability of the TM rats regenerated with the 3D chitosans scaffolds was recovered. Color images available online at www.liebertonline.com/tea

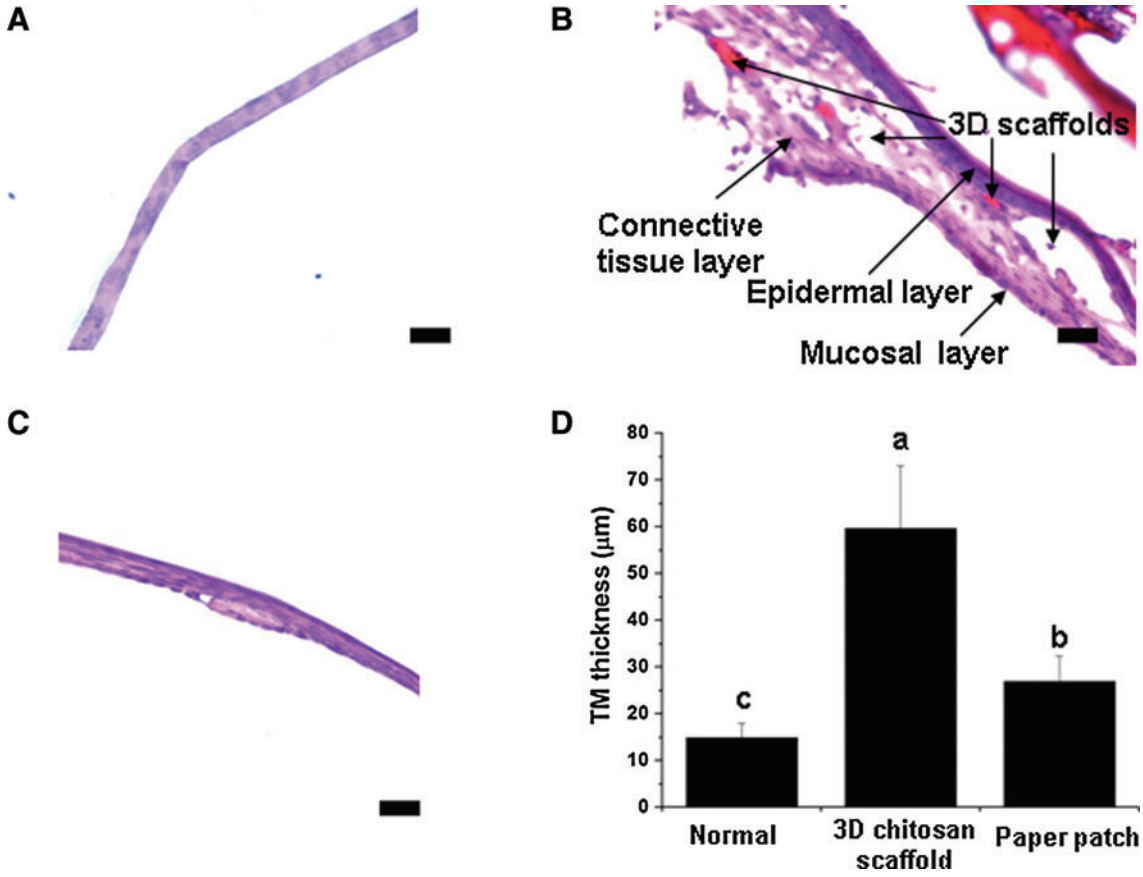

FIG. 5. Histological observation study. Histological section of **(A)** normal TM, **(B)** TM regenerated with 3D chitosan scaffold, and **(C)** TM regenerated with paper patch. **(D)** Quantification of the average TM thickness of the regenerated TMs ("a–c" mean that average TM thickness of regenerated TMs is significantly different among different characters [$p < 0.05$, $n = 3$ for each group, hematoxylin and eosin images]). Scale bar = 25 μm. Color images available online at www.liebertonline.com/tea

there was no perfect TM regeneration in both the 3D chitosan-treated and the paper patch-treated group, although we observed keratin layers in the 3D chitosan scaffold-treated groups (Fig. 4D). After 7 days, 6 (60%) TMs showed complete regeneration. Meanwhile, in the paper patch group (as a control group), only 1 (10%) TMs showed no perforation. There was a statistically significant difference in the healing ratio at 1 week between the two groups ($p = 0.02$). After 10 days, the TMs regenerated perfectly of the 3D chitosan-treated and paper patch-treated group were 8 (80%) TMs and 7 (70%) TMs, respectively ($p = 0.50$). All the TMs were healed completely in 2 weeks. These results showed that the 3D chitosan scaffold as an artificial TM accelerated TM healing as well as fast healing time compared with the paper patches.

For checking healing status, we measured healing sensitivities using ABR thresholds. The average auditory threshold of the normal TMs of rats was 23.3 ± 2.5 dB (Fig. 4O, $n = 10$). After perforation of TMs of rats, the average auditory threshold was 53.8 ± 7.5 dB (Fig. 4P, $n = 4$). We checked the ABR after TM regeneration using the 3D chitosan scaffold. The average auditory threshold of the TMs of rats with 3D chitosan scaffold-treated was 24.6 ± 6.6 dB (Fig. 4Q, $n = 10$). There was no significant difference in hearing status between scaffold-treated TMs and normal TMs ($p = 0.543$), indicating that the 3D chitosan scaffolds stimulated TM regeneration.

Histological examination was conducted on TMs regenerated with the 3D chitosan scaffolds and the paper patches. Figure 5B shows the representative histological section of the TM regenerated with the 3D chitosan scaffold. The epidermal layer, connective tissue layer, and mucosal layer were viable, although they showed irregular gross feathers compared with the normal TM (Fig. 5A). We also observed many empty spaces in the regenerated TM cells that were considered as the 3D chitosan scaffolds and pore spaces. The scaffold materials were easily lost during the tissue processing for staining. Paper patch-treated TMs (Fig. 5C) showed thinner eardrums compared with TMs regenerated with the 3D chitosan scaffolds. The TMs were also detected with abnormal findings such as granulation or scar tissues.

Compared with the normal TMs (Fig. 5A) or TMs regenerated with paper patch (Fig. 5C), the average thickness of the TMs regenerated with the 3D chitosan scaffolds was greater than paper patches ones or normal TMs. However, this result demonstrated that the 3D chitosan scaffolds provided the environment for TM regeneration. After 5 weeks, to evaluate the quality of the regenerated TMs with the 3D chitosan scaffolds, we performed the TEM observation. The TMs regenerated with the 3D chitosan scaffold showed thick tissues with irregular outer epidermal layers with keratin and loss of circular fibrous layers (Fig. 6B); whereas normal, unperforated TMs showed thin compact tissues composed of

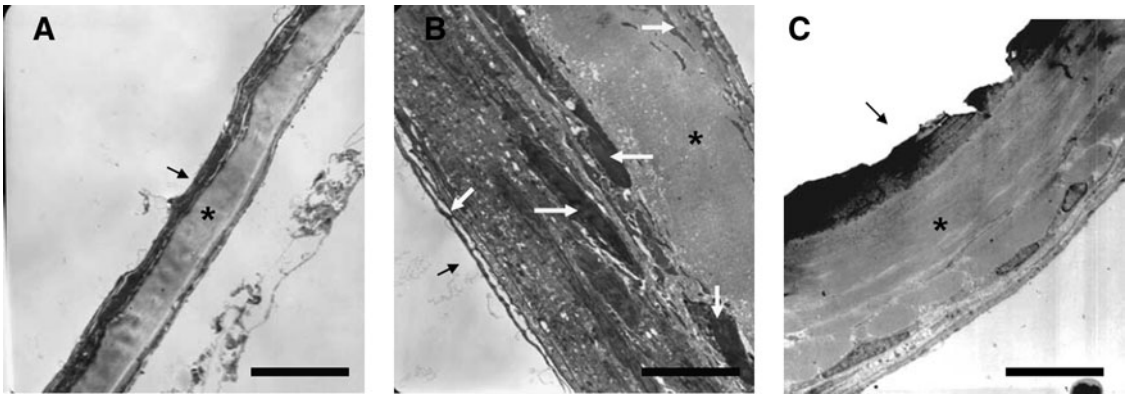

FIG. 6. TEM findings of regenerated TMs. TEM images of **(A)** normal TM and **(B)** TM regenerated with 3D chitosan scaffold, and **(C)** TM regenerated with paper patch; the TEM images indicate that regenerated TM using the 3D chitosan scaffold had outer epidermal layers with keratin, lamina propria (*) and remained 3D scaffolds (white arrow) as well as larger TM thickness than a normal TM. Black arrows indicate outer epidermal layer. Scale bar = 25 μm. TEM, transmission electron microscopy.

an outer epidermal layer, radiate and circular fibrous layers of lamina propria, and an inner mucosal layer (Fig. 6A). The TMs regenerated with the paper patch also showed heavier thickness than those with normal TMs (Fig. 6C). We were able to observe that the 3D chitosan scaffold remained inside the regenerated TMs in FESEM and histologic findings. Since we used water-insoluble chitosan as a main material of our novel artificial TMs, this finding was absolutely expected. Water-insoluble chitosan scaffolds cannot be dissolved in the outer ear for several weeks.

Our histological examination studies showed that the TM cells, including keratinocytes and fibroblasts, are regenerated along the surface and inner pores of the 3D chitosan scaffolds although the TM regenerated with the 3D chitosan scaffolds had thick thickness compared with normal TMs and the regenerated TMs with paper patch. However, we observed that the cells along the 3D chitosan scaffolds were well-organized parallel to the original TM direction, indicating that the 3D chitosan scaffolds is viable as a new healing method for TM perforations.

Possible exposures of infection, bacteria, or even foreign bodies were issued by the porous structure of the 3D chitosan scaffold compared with other regular or smooth surface structures. In this study, we observed that almost the TMs perforated were regenerated with the 3D chitosan scaffolds within 1 week, and complications such as bacterial or foreign body infection did not occur to any of the cases. The chitosan as a main biomaterial for the artificial TM has a good antibacterial property due to its unique molecular structure and amine groups so that the 3D chitosan scaffolds may prevent the infection with bacterial and foreign bodies themselves.[21–23] With these findings, we may conclude that the 3D chitosan scaffolds could provide a good antibacterial environment, although they have porous surfaces.

As previously mentioned, TM perforations, in cases of both acute and chronic hearing loss, are common problems in the world. Surgical treatments or the paper patch graft technique are still used to heal TM perforations, despite their many disadvantages. We have attempted a novel therapy using 3D chitosan scaffolds for TM regeneration. In this study, we tested the 3D chitosan scaffold as a new artificial TM in an animal model of rats with acute TM perforations and showed that TM perforations healed better when the 3D chitosan scaffolds were used than when the TMs healed with paper patch, indicating that the 3D chitosan scaffolds are potentially a viable alternative to surgical treatments or paper patch graft techniques. Our group recently developed a method to create a chronic TM animal model.[27] These animal models will provide us with effects of the 3D chitosan scaffolds to study the chronic TM regeneration for our future study. Finally, the results of this study demonstrated that the 3D chitosan scaffolds are very effective for acute TM regeneration and provided us with information for better understanding chronic TM regeneration for future studies. The 3D chitosan scaffold, an alternative to surgical treatment or the paper patch graft technique, has high potential for treating TM perforations.

Conclusions

In this study, we developed a novel healing method for TM perforation as a viable alternative to surgical treatment or the paper patch graft technique. Various constituent 3D chitosan scaffolds were prepared, and the 3D chitosan scaffold of 5 wt.% chitosan was considered optimal as an artificial TM. The 5 wt.% chitosan 3D chitosan scaffolds showed good *in vitro* TM cell viability, as well as the suitable structure properties for an artificial TM. *In vivo* studies showed that the 3D chitosan scaffold accelerated TM regeneration than paper patch. The regenerated TM with the 3D chitosan scaffold had epidermal layer, connective tissue layer, mucosal layer, and the remaining scaffold, although they were thick compared with normal TMs. We conclude that this 3D chitosan scaffold technique is an effective, viable method as a new healing method for TM perforations.

Acknowledgments

This study was supported by a grant from the Korea Health Technology R&D Project, Ministry for Health, Welfare and Family Affairs, Republic of Korea (A090869). The authors thank the National Instrumentation Center for Environmental Management (NICEM) for providing FESEM measurement.

Disclosure Statement

No competing financial interests exist.

References

1. Gladstone, H.B., Jacker, R.K., and Varav, K. Tympanic membrane wound healing: an overview. Otolaryngol Clin North Am **28,** 913, 1995.
2. Laidlaw, D.W., Costantino, P.D., Govindaraj, S., Hiltzik, D.H., and Catalano, P.J. Tympanic membrane repair with a dermal allograft. Laryngoscope **111,** 702, 2001.
3. Kim, J.H., Choi, S.J., Park, J.S., Lim, K.T., Choung, P.H., Kim, S.W., Lee, J.B., Chung, J.H., and Choung, Y.H. Tympanic membrane regeneration using a water-soluble chitosan patch. Tissue Eng Part A **16,** 225, 2010
4. Blake, C.J. Transactions of the First of Congress of the International Otological Society (abstract). New York: D. Appleton and Co., 1887, p. 125.
5. Chun, S.H., Lee, D.W., and Shin, J.K. A clinical study of traumatic tympanic perforation. Korean J Otolaryngol **23,** 437, 1999.
6. Bonzona, N., Carrat, X., Deminiere, C., Daculsi, G., Lefebvre, F., and Rabaud, M. New artificial connective matrix made of fibrin monomers, elastin peptides and type I+III collagens: structural study, biocompatibility and use as tympanic membranes in rabbit. Biomaterials **16,** 881, 1995.
7. Chauvin, K., Bratton, C., and Parkins, C. Healing large tympanic membrane perforations using hyaluronic acid, basic fibroblast growth factor, and epidermal growth factor. Otolaryngol Head Neck Surg **121,** 43, 1999.
8. Kohn, F.E., Feijen, J., and Feenstra, L. New perspectives in myringoplasty. Int J Artif Organs **7,** 151, 1984.
9. Weber, D.E., Semaan, M.T., Wasman, J.K., Beane, R., Bonassar, L.J., and Megerian, C.A. Tissue-engineered calcium alginate patches in the repair of chronic chinchilla tympanic membrane perforations. Laryngoscope **116,** 700, 2006.
10. Ghassemifar, R., Redmond, S., Zainuddin, and Chirila, T.V. Advancing towards a tissue-engineered tympanic membrane: silk fibroin as a substratum for growing human eardrum keratinocytes. J Biomater Appl **24,** 591, 2010.
11. Kim, J., Kim, C.H., Park, C.H., Seo, J.N., Kweon, H.Y., Kang, S.W., and Lee, K.G. Comparison of methods for the repair of acute tympanic membrane perforations: silk patch vs. paper patch. Wound Repair Regen **18,** 132, 2010.
12. Kim, J.H., Bae, J.H., Lim, K.T., Choung, P.H., Park, J.S., Choi, S.J., Im, A.L., Lee, E.T., Choung, Y.H., and Chung, J.H. Development of water-insoluble chitosan patch scaffold to repair traumatic tympanic membrane perforations. J Biomed Mater Res A **90,** 446, 2009.
13. Parekh, A., Mantle, B., Banks, J., Swarts, J.D., Badylak, S.F., Dohar, J.E., and Hebda, P.A. Repair of the tympanic membrane with urinary bladder matrix. Laryngoscope **119,** 1206, 2009.
14. Lim, A.A., Washington, A.P., Greinwald, J.H., Lassen, L.F., and Holterl, M.R. Effect of pentoxifyline on the healing of guinea pig tympanic membrane. Ann Otol Rhinol Laryngol **109,** 262, 2000.
15. Hakuba, N., Iwanaga, M., Tanaka, S., Hiratsuka, Y., Kumabe, Y., Konishi, M., Okanoue, Y., Hiwatashi, Y., and Wada, T. Basic fibroblast growth factor combined with atelocollagen for closing chronic tympanic membrane perforations in 87 patients. Otol Neurtol **31,** 118, 2010.
16. Hott, M.E., Megerian, C.A., Beane, R., and Bonassar, J. Fabrication of tissue engineered tympanic membrane patches using computer-aided design and injection modeling. Laryngoscope **114,** 1290, 2004.
17. Deng, Z., Wu, J., Qiu, J., Wang, J., Tian, Y., Li, Y., and Jin, Y. Comparison of porcine acellular dermis and dura mater as natural scaffolds for bioengineering tympanic membranes. Tissue Eng Part A **15,** 3729, 2009.
18. Ungea, M.V., Dirckxb, J., and Olivius, N.P. Embryonic stem cells enhance the healing of tympanic membrane perforations. Int J Pediatr Otorhinolaryngol **67,** 215, 2003.
19. Rahman, A., Unge, M.V., Olivius, P., Dirckx, J., and Hultcrantz, M. Healing time, long-term result and effects of stem cell treatment in acute tympanic membrane perforation. Int J Pediatr Otorhinolaryngol **71,** 1129, 2007.
20. Rahman, A., Olivius, P., Dirckxb, J., Unge, M.V., and Hultcrantz, M. Stem cells and enhanced healing of chronic tympanic membrane perforation. Acta Otolaryngol **128,** 352, 2008.
21. Kim, I.Y., Seo, S.J., Moon, H.S., Park, I.Y., Kim, B.C., and Cho, C.S. Chitosan and its derivatives for tissue engineering applications. Biothechnol Adv **26,** 1, 2008.
22. Rinaudo, M. Chitin and chitosan: properties and applications. Prog Polym Sci **31,** 603, 2006.
23. Chen, C.L., Wang, Y.M., Liu, C.F., and Wang, J.Y. The effect of water-soluble chitosan on macrophage activation and the attenuation of mite allergen-induced airway inflammation. Biomaterials **29,** 2173, 2008.
24. Madihally, S.V., and Matthew, W.T. Porous chitosan scaffolds for tissue engineering. Biomaterials **20,** 1133, 1999.
25. Huang, Y., Onyeri, S., Siewe, M., Moshfeghian, A., and Madihally, S.V. *In vitro* characterization of chitosan-gelatin scaffolds for tissue engineering. Biomaterials **26,** 7616, 2005.
26. Hsieh, W.C., Chang, C.P., and Lin, S.M. Morphology and characterization of 3D micro-porous structured chitosan scaffolds for tissue engineering. Colloids Surf B Biointerfaces **57,** 250, 2007.
27. Choi, S.J., Kim, W.S., Kim, J.H., Lee, J.B., Choo, O.S., Chung, J.H., and Choung, Y.H. Efficient treatment of chronic tympanic membrane perforations in animal models by chitosan patch scaffolds. Tissue Eng Regen Med **8,** 141. 2011.

Address correspondence to:
Yun-Hoon Choung, D.D.S., M.D., Ph.D.
Department of Otolaryngology
Ajou University School of Medicine
Suwon 443-721
Republic of Korea

E-mail: yhc@ajou.ac.kr

Jong Hoon Chung, Ph.D.
Department of Biosystems & Biomaterials
Science and Engineering
Seoul National University
Seoul 151-742
Republic of Korea

E-mail: jchung@snu.ac.kr

Received: September 7, 2010
Accepted: June 17, 2011
Online Publication Date: July 27, 2011